

Experimental Verification of a Leaky-Wave Antenna Based on Bianisotropic Huygens' Metasurface

Elena Abdo-Sánchez¹, Michael Chen², Ariel Epstein³ and George V. Eleftheriades²,

¹Dpto. Ingeniería de Comunicaciones, E.T.S.I. Telecomunicación, Universidad de Málaga, Andalucía Tech, E-29071 Málaga, Spain, e-mail: elenaabdo@ic.uma.es

²The Edward S. Rogers Sr. Department of Electrical and Computer Engineering University of Toronto, Toronto, Canada

³Andrew and Erna Viterbi Faculty of Electrical Engineering, Technion - Israel Institute of Technology, Haifa 32000, Israel

Abstract—In this communication, the experimental verification of a leaky-wave antenna that uses a Huygens' metasurface to have a control on the radiation parameters is addressed. The antenna consists of a parallel-plate waveguide in which the top plate has been replaced by an omega-type bianisotropic Huygens' metasurface, in order to transform the guided mode into the desired leaky-mode with arbitrary choice of the leakage rates, pointing direction and waveguide height. The physical implementation of the metasurface is explained. Two design examples, radiating at broadside with different leakage factors, are implemented, manufactured and measured. Simulated and experimental results of the achieved directivity, scanning performance and radiation patterns are provided, experimentally corroborating the concept.

Index Terms—bianisotropy, Huygens' metasurface, leaky-wave antenna, measurement, radiation.

I. INTRODUCTION

Leaky-wave antennas (LWAs) are receiving increasing attention as a cost-effective solution for the emerging communication systems that demand a simple, low-profile and low-cost antenna technology with beam scanning capabilities. They consist of a waveguiding structure that radiates power gradually while the guided mode is being propagated along it. The radiation characteristics are intrinsically related to the propagation constant of the resulting leaky-mode. The phase constant, β , determines the pointing angle, whereas the attenuation constant α , named *leakage factor*, determines the directivity. It is then interesting to achieve an independent control of both parameters to be able to accomplish a certain radiation pattern.

Metasurfaces are the two-dimensional version of metamaterials and have allowed the demonstration of anomalous physical phenomenons. Specifically, Huygens' metasurfaces have shown to be a powerful tool to achieve almost arbitrary electromagnetic field transformations [1]–[3]. They consist of an array of collocated polarizable electric and magnetic dipoles that are designed to make the boundary condition fulfilled. Recently, the authors have proposed a novel concept of LWA based on a parallel-plate waveguide with the top plate being a bianisotropic Huygens' metasurface that allows a wide control of the radiation parameters [4], [5]. In this communication, the implementation and experimental validation of this concept are addressed.

II. CONCEPT

The proposed antenna consists of a parallel-plate waveguide in which the top plate has been replaced by an omega-type bianisotropic Huygens' metasurface (O-BMS). A metasurface with bianisotropy is used since it was demonstrated it allows arbitrary field transformation with passive and lossless unit-cells when just one condition is fulfilled: local power conservation [6]. The extra degree of freedom provided by the magnetoelectric coupling allows the control of both the reflection and transmission coefficients in the metasurface, required to build a LWA with control of the radiation pattern. Fig. 1 shows the schematic of the proposed concept.

Let us assume a transverse electric (TE) polarized field as excitation ($E_y = E_z = H_x = 0$). Then, the transverse field components above (E_x^+ and H_y^+) and below (E_x^- and H_y^-) the O-BMS are related through the bianisotropic sheet transition conditions [7]:

$$\begin{aligned} \frac{1}{2}(E_x^+ + E_x^-) &= -Z_{se}(H_y^+ - H_y^-) - K_{em}(E_x^+ - E_x^-) \\ \frac{1}{2}(H_y^+ + H_y^-) &= -Y_{sm}(E_x^+ - E_x^-) + K_{em}(H_y^+ - H_y^-) \end{aligned} \quad (1)$$

where Z_{se} stands for the electric surface impedance, Y_{sm} for the magnetic surface admittance and K_{em} for the magnetoelectric coupling coefficient.

The electromagnetic field inside the waveguide that fulfills Maxwell's equations is estipulated as follows [4], [5]:

$$E_x^- = |E_{in}|(e^{jk_z^-(z+d)} - e^{-jk_z^-(z+d)})e^{-jk_y^-y}. \quad (2)$$

For the region above the metasurface, a leaky mode is desired. Therefore, the following electric field is stipulated:

$$E_x^+ = |E_{out}|e^{-jk_z^+z}e^{-jk_y^+y}. \quad (3)$$

In both regions, the propagation constants of the fields are complex:

$$\begin{aligned} k_y^- &= \beta^- - j\alpha; \quad k_z^- = \beta_z^- - j\alpha_z^-; \quad k^{-2} = k_y^{-2} + k_z^{-2} \\ k_y^+ &= \beta^+ - j\alpha; \quad k_z^+ = \beta_z^+ - j\alpha_z^+; \quad k^{+2} = k_y^{+2} + k_z^{+2}. \end{aligned} \quad (4)$$

It was demonstrated in [4], [5] that the only restriction (imposed by the local power conservation condition) to get the desired field transformation is that the field below and above the metasurface has the same decay rate (α) along y : $\alpha^+ = \alpha^-$. Then, it is possible to get arbitrary control of the following parameters:

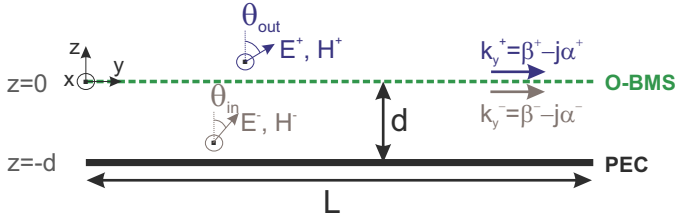


Fig. 1. Proposed concept schematic.

- Waveguide height: d , even below the cut-off frequency of the equivalent parallel-plate waveguide.
- Phase constant below the metasurface, β^- , which determines θ_{in} .
- Phase constant above the metasurface, β^+ , which determines θ_{out} .
- Leakage factor $\alpha = \alpha^+ = \alpha^-$, which determines the directivity.

When α is constant, the resulting metasurface is periodic, so that the pointing beam corresponds to either the harmonic $m = 1$ or $m = -1$. It was shown that, even for long periodicities, only this Floquet mode is excited, even if, according to Floquet's theorem, other Floquet modes are generated. Therefore, it is worth mentioning that the metasurface achieves an automatic suppression of the spurious Floquet modes to guarantee that the radiated field is the one stipulated [5].

III. PHYSICAL IMPLEMENTATION

Once the desired parameters for the fields (θ_{in} or the period, θ_{out} and α) and the waveguide height (d) have been set, the metasurface constituents $\{K_{em}, Z_{se}, Y_{sm}\}$ can be calculated. Then, the first step to find an implementation of the metasurface is to sample the parameters with the length along y of the unit-cell that will be used to build the metasurface. A sampling rate of $\frac{\lambda_0}{6}$ (a value that has been previously shown to allow the homogenization approximation) has been chosen.

At each point $y = y_0$, the local properties of the metasurface can be approximated by the scattering properties of an infinite periodic array (local periodicity assumption). In this way, each unit-cell can be characterized by a 2×2 impedance matrix $[\mathbf{Z}]$ that relates the tangential fields below and above the metasurface [8]:

$$\begin{pmatrix} E_x^- \\ E_x^+ \end{pmatrix} = \begin{pmatrix} Z_{11} & Z_{12} \\ Z_{21} & Z_{22} \end{pmatrix} \begin{pmatrix} H_y^- \\ -H_y^+ \end{pmatrix}. \quad (5)$$

By using (1), the impedance matrix in terms of the metasurface parameters can be expressed as follows [6]:

$$\begin{aligned} Z_{11} &= Z_{se} + \frac{(1 + 2K_{em})^2}{4Y_{sm}} \\ Z_{12} = Z_{21} &= Z_{se} - \frac{(1 - 2K_{em})(1 + 2K_{em})}{4Y_{sm}} \\ Z_{22} &= Z_{se} + \frac{(1 - 2K_{em})^2}{4Y_{sm}}. \end{aligned} \quad (6)$$

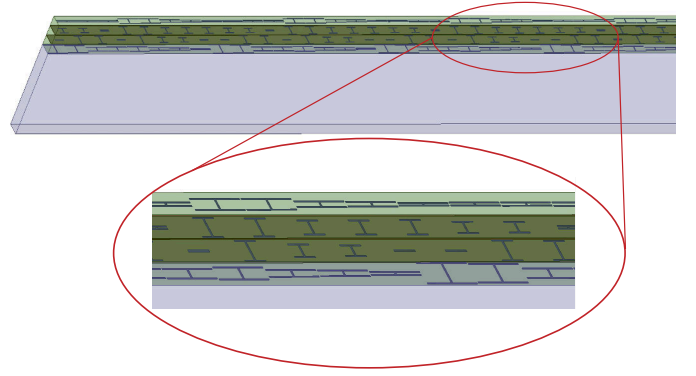


Fig. 2. Physical implementation for the prototype of the LWA.

For the implementation of each unit-cell, a structure of three dielectric laminates with four copper trace layers has been used. The substrate chosen for the designs was 50 mil-thick RO3010 and the laminates were bonded by Rogers 2 mil-thick 2929 bondply. The dog-bone geometry was chosen for the copper traces, since they allowed a wide range of reactance values (from capacitive to inductive behavior) to be synthesized by modifying its length. Fig. 2 shows part of the resulting physical implementation of the antenna for a certain design. The reason to use four layers instead of three (which is customary in this kind of metasurfaces) is to have an extra degree of freedom to reduce the total losses of the unit-cell and, then, obtain an impedance matrix closer to the theoretical one given by (6).

IV. RESULTS

Two designs have been carried out at 20 GHz. In both of them, a period of $8/6\lambda_0$, $d = 0.75\lambda_0$ and broadside radiation ($\theta_{out} = 0^\circ$) have been arbitrarily chosen. Different leakage factors have been selected to demonstrate the control of the radiation parameters (in this case, the directivities). In this way, one design has $\alpha = 0.02k_0$ and length $L = 10\lambda_0$ and the other one $\alpha = 0.013k_0$ and $L = 15\lambda_0$, so both theoretically radiate around 90% of the input power. The magnitudes of the electric fields along the zy -plane obtained from the electromagnetic simulation using ANSYS HFSS of the physical implementations for the two designs are plotted in Fig. 3. The transformation of the guided mode into the leaky-mode in the broadside direction can be observed. The different leakage rates can be also noticed in the field decay rates inside the waveguide.

A photograph of one of the prototypes is shown in Fig. 4. The waveguide was fabricated on a 4 mm Aluminium block and manufactured in two pieces (split along the longitudinal axis) in a similar way as done in [9]. Then, the structure was assembled using metallic screws. A SMA connector with an exposed pin along the x -direction was used to feed the structure as a TE current source.

Fig. 5 shows the measured 2D directivity (the directivity considering only the zy -plane) as a function of both the frequency and the angle for both designs. The same main beam

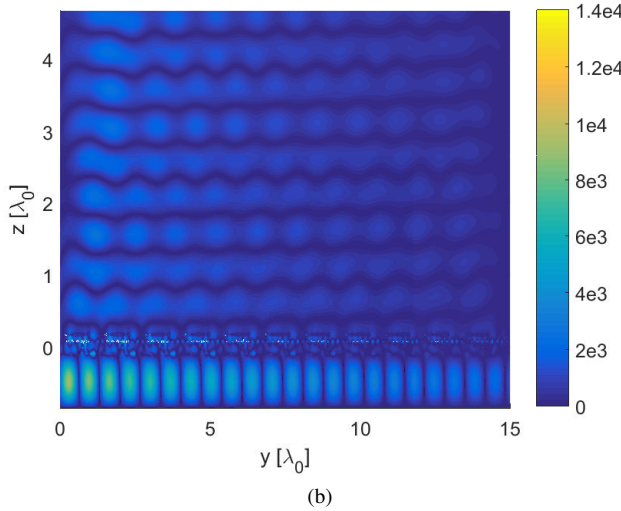
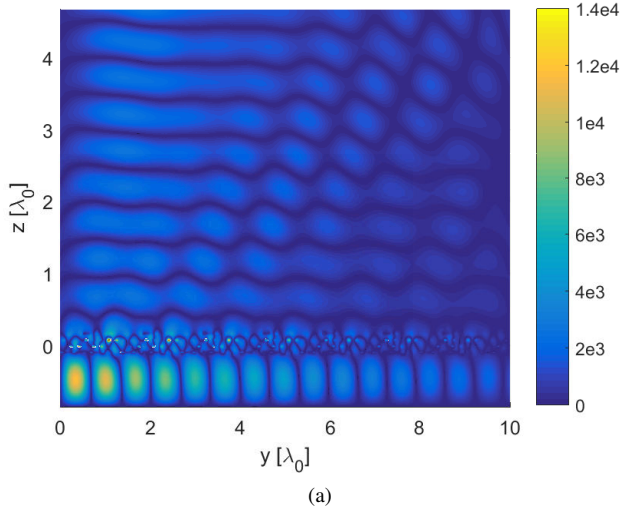


Fig. 3. Field distributions $|Re(E_x(y, z))|$ (V/m) for input power of 1W over a waveport area $\lambda_0/6 \times \lambda_0/9.5 \times 0.75\lambda_0$. (a) Design with $\alpha = 0.02k_0$ and (b) design with $\alpha = 0.013k_0$.

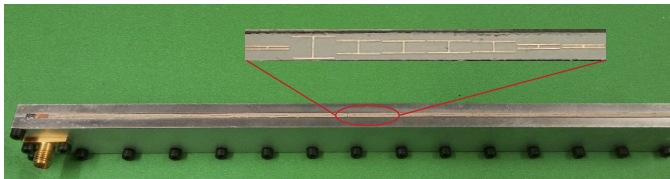


Fig. 4. Photograph of one of the prototypes.

direction and similar radiation patterns are observed in both designs. It can be noticed that the two designs have a slow scanning rate with frequency. Since both designs only differ in the leakage factor values (directivity), the similarities in the two plots are a good indicator. It can be seen that the frequency at which the side-lobe (spurious Floquet modes) suppression is almost achieved do not coincide with the design frequency

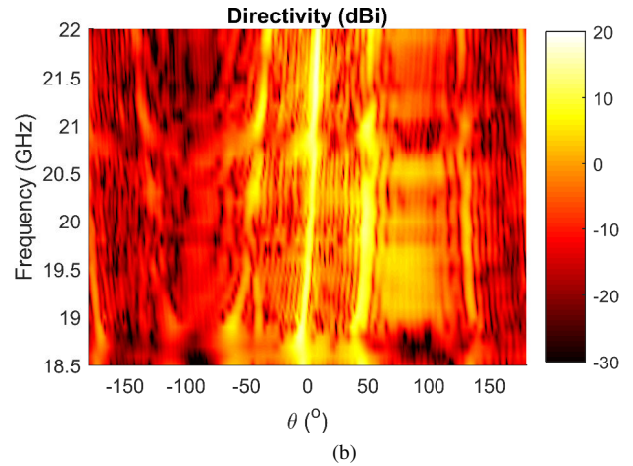
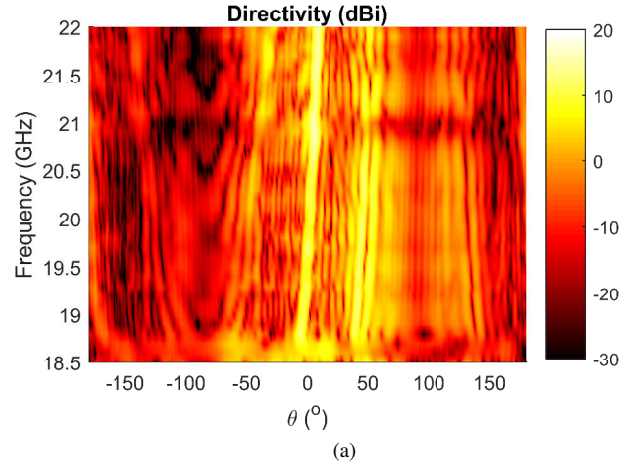


Fig. 5. Measured 2D directivities as a function of the frequency and the angle for both designs. (a) Design with $\alpha = 0.02k_0$ and (b) design with $\alpha = 0.013k_0$.

(20 GHz), but it is shifted to around 21 GHz in the first design and around 21.5 GHz. Please note that these frequencies also coincide with those at which the maximum value of the directivities occur. The directivity values are slightly higher in the second design as targeted. In order to observe these results clearer, Fig. 6 shows the measured maximum 2D directivity as a function of frequency for the two designs. It can be noticed that the prototype with lower leakage rate achieves a maximum directivity of around 18 dBi, which is close to the obtained value from electromagnetic simulations using *ANSYS HFSS* (18.7 dBi) and reasonable with respect to the ideal theoretical value (19.3 dBi). Likewise, the design with the highest α has a maximum directivity of around 16 dBi, which agrees with the achieved value in simulation (16.7 dBi) and is slightly lower than the theoretical value (17.3 dBi) as expected due to the undesired losses. Therefore, it is experimentally demonstrated that it is possible to control the leakage rate independently on the pointing direction with the proper design of the metasurface.

It has been found that the source for the frequency shift of

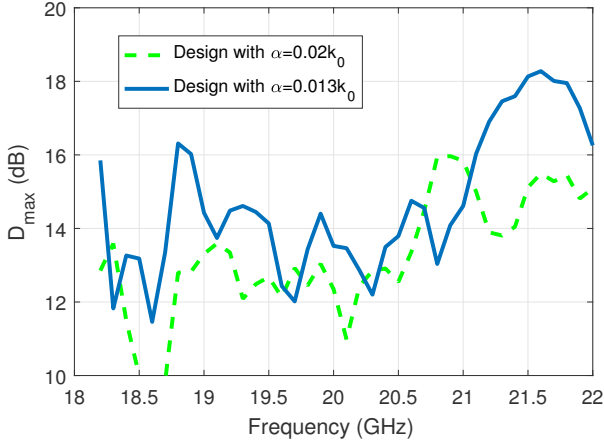


Fig. 6. Measured maximum 2D directivity as a function of frequency for the two fabricated designs.

the measurements with respect to the design is likely due to the apparent value of the permittivity of the RO3010 substrate, which seems to differ from the nominal value provided by the manufacturer (12.94 at 20 GHz). Simulations have been carried out introducing a decrease in the permittivity of the substrate and, for a 15% of deviation, good agreement with the measurements has been found. Fig. 7 shows, for the two designs, the radiation pattern comparison between measurement and simulation with the permittivity deviation of 15% at the frequency around which the maximum directivity and suppression of side lobes are achieved. Slightly higher side lobes are obtained in the experimental results; however, overall good agreement is observed. The radiation patterns for the two designs are similar but with different directivities due to the different leakage factors, thus corroborating the experimental verification of the concept. Due to the frequency shift because of the permittivity deviation, the radiation patterns do not have the maximum at broadside.

If it is assumed that the found permittivity deviation in the substrate of the metasurface does not significantly modify the field inside the waveguide, it is expected that the pointing direction is the same as for the design (since the periodicity of the metasurface should be the designed one in the fabricated prototype). To corroborate this conclusion, Fig. 8 shows the variation with frequency of the pointing angle of the central beam of the radiation pattern for the design with $\alpha = 0.013k_0$. Measurement and electromagnetic simulations with and without permittivity deviations are plotted. A very good agreement between the measurement and both simulations can be observed. Therefore, the pointing direction is not very much affected by the permittivity deviation, so broadside is obtained at the designed frequency (20 GHz). However, at this frequency, the metasurface is not behaving as targeted and the side lobe suppression is achieved at a shifted frequency as previously shown, which corresponds to a low positive pointing angle. It can be again noticed that the scanning rate is rather slow. The small pointing deviation in the measured

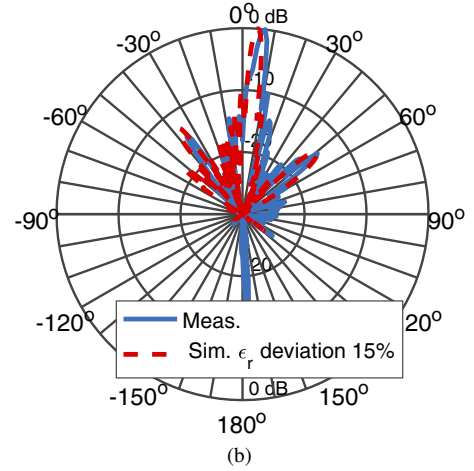
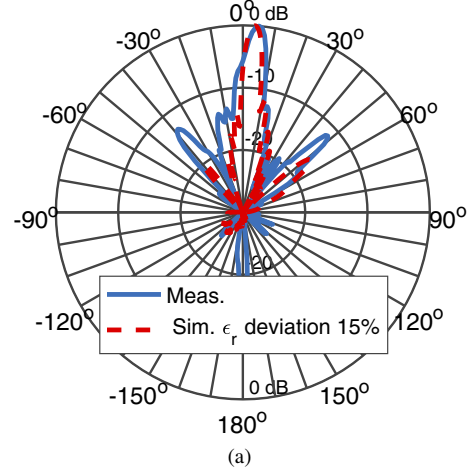


Fig. 7. Comparison of the radiation patterns from measurements and simulations considering a permittivity deviation for the substrate of 15%. (a) Design with $\alpha = 0.02k_0$ at 21 GHz and (b) design with $\alpha = 0.013k_0$ at 21.5 GHz.

values with respect to simulations can be attributed to some minor miscalibration when performing the anechoic chamber measurements.

V. CONCLUSION

It has been shown that the physical implementation of the bianisotropic Huygens' metasurface can be achieved using printed dog-bones on bonded three dielectric laminates, being compatible with PCB fabrication. In this way, two prototypes of a LWA based on bianisotropic Huygens' metasurface have been manufactured and measured, in order to show the control of the radiation pattern that this innovative antenna topology allows. The waveguide has been built as a metallic cavity with a slit on the top in which the metasurface has been placed. Specifically, the designs are chosen to show arbitrary different leakage factors with the same pointing direction (broadside in this case). A deviation in the frequency at which the metasurface achieves the stipulated field transformation (with suppression of spurious Floquet modes) is found, which is shown to be caused by a deviation in the substrate permittivity

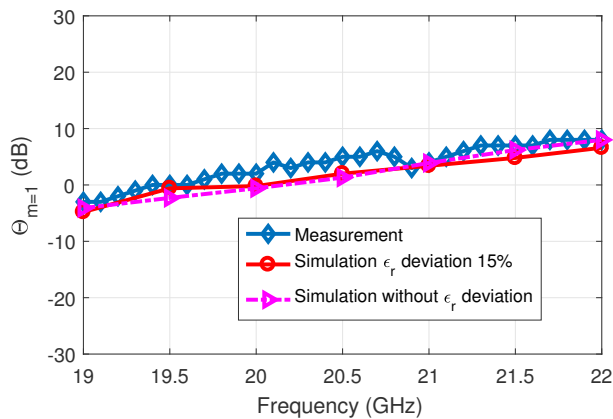


Fig. 8. Pointing angle of the central beam (corresponding to the spatial harmonic $m = 1$) as a function of frequency for the design of $\alpha = 0.013k_0$. Measurement results and simulations with the nominal value of ϵ_r , as well as with a value a 15% lower than the nominal value are plotted.

from the value provided by the manufacturer. In any case, the mitigation of spurious Floquet modes with the result of mainly a single beam (very low side lobes) has been experimentally shown. It is also demonstrated that the radiation patterns for the two designs are similar (same pointing direction) but with different directivities. The values of the directivities agree with those obtained from the electromagnetic simulation and the chosen leakage factors. Therefore, it has been experimentally verified that, by properly designing the metasurface, two different designs with the same pointing angle but different leakage rates can be realized. Then, independent control of the leakage factor and pointing direction can be achieved.

ACKNOWLEDGMENT

This project has received funding from the European Union's Horizon 2020 research and innovation programme under the Marie Skłodowska-Curie grant agreement No 706334.

REFERENCES

- [1] C. Pfeiffer and A. Grbic, "Metamaterial Huygens surfaces: tailoring wave fronts with reflectionless sheets," *Phys. Rev. Lett.*, vol. 110, no. 19, pp. 197401, May 2013.
- [2] F. Monticone, N. M. Estakhri, and A. Alù, "Full control of nanoscale optical transmission with a composite metascreen," *Phys. Rev. Lett.*, vol. 110, no. 20, p. 203903, May 2013.
- [3] M. Selvanayagam and G. V. Eleftheriades, "Discontinuous electromagnetic fields using orthogonal electric and magnetic currents for wavefront manipulation," *Opt. Express*, vol. 21, no. 12, pp. 14 409–14 429, Jun. 2013.
- [4] E. Abdo-Sánchez, A. Epstein and G. V. Eleftheriades, "Bianisotropic Huygens' metasurface leaky-wave antenna with flexible design parameters," *11th European Conference on Antennas and Propagation (EUCAP)*, Paris, 2017, pp. 3315–3318.
- [5] E. Abdo-Sánchez, M. Chen, A. Epstein and G. V. Eleftheriades, "A Leaky-Wave Antenna With Controlled Radiation Using a Bianisotropic Huygens Metasurface," to be published in *IEEE Trans. Antennas Propag.*.
- [6] A. Epstein and G. V. Eleftheriades, "Arbitrary power-conserving field transformations with passive lossless Omega-type bianisotropic metasurfaces," *IEEE Trans. Antennas Propag.*, vol. 64, no. 9, pp. 3880–3895, Sept. 2016.

- [7] Y. Ra'di and S. A. Tretyakov, "Balanced and optimal bianisotropic particles: Maximizing power extracted from electromagnetic fields," *New J. Phys.*, vol. 15, no. 5, p. 053008, 2013.
- [8] M. Selvanayagam and G. V. Eleftheriades, "Circuit modeling of Huygens surfaces," *IEEE Antennas Wireless Propag. Lett.*, vol. 12, no. 12, pp. 1642–1645, 2013.
- [9] A. Epstein, J. P. S. Wong, G. V. Eleftheriades, "Cavity-excited Huygens metasurface antennas for near-unity aperture illumination efficiency from arbitrarily large apertures," *Nature Commun.*, vol. 7, Jan. 2016.